Understanding the Movement, Encapsulation, and Energy Barrier of Water Molecule Diffusion into and in Silicalites Using Ab Initio Calculations

C. Bussai,[†,‡] S. Hannongbua,*[,†] and R. Haberlandt[‡]

Department of Chemistry, Faculty of Science, Chulalongkorn University, Bangkok 10330, Thailand, and Department of Molecular Dynamics and Computer Simulations, Institute for Theoretical Physics (ITP), Faculty of Physics and Geoscience, University of Leipzig, Augustusplaz 10-11, 4109, Leipzig, Germany

Received: September 17, 2000; In Final Form: January 26, 2001

Quantum chemical calculations at the Hartree-Fock and MP2 levels have been performed to investigate water−silicalite interactions as well as the energy barrier and water orientations during diffusion into and in silicalite. Experimental geometries of water and silicalite have been used and kept constant throughout. The silicalite crystal structure has been represented by three fragments consisting of 20, 52, and 64 heavy atoms (oxygen and silicon atoms). Calculations have been performed using extended 6-31G and 6-31G* basis sets with BSSE (basis set superposition error) corrections. The results indicate obviously how the water molecule moves and turns via diffusion through the center of the silicalite pore in order to find the optimal route. The energy barriers for the water molecule to enter the pore and to diffuse from one channel to another have been clearly examined. The most stable binding site inside the pore is to be encapsulated in the intersection channel. It was also found that a water molecule enters and leaves the pores by pointing its dipole vector toward the center of the cavity.

1. Introduction

Zeolites[1,2] are outstanding among the interesting materials for chemical science and technology for their special characteristics and multifarious uses. Their active sites appear on the microporous inner wall positions. The size of the micropore or cavity plays an important role in the selectivity process. The widespread and diverse uses of zeolites are as catalysts and molecular sieves in the chemical industry and as ion exchangers, in particular as absorbents in detergents.[3−5] Diffusion phenomena,[6] which are the basis of those applications, lie in the adsorption and the transportation processes.[7,8] Interest in the water−zeolite interaction arises from the fact that water plays strong and essential roles for both absorption and catalytic properties of zeolite,[9,10] as it is known that all natural zeolites are hydrated. In addition, water molecules facilitate the exchange of the charge-compensating cations, which are essential for the industrial catalysts. Therefore, understanding the water−zeolite interactions as well as the behavior of water in zeolite, especially in relation with the zeolite structure, would lead to rapid development of the knowledge in this field, and hence of the application of the zeolites.

According to our best knowledge, the only available data on the water−silicalite interactions are the experimental measurements by Flanigen et al.[11] and Vigne-Maeder et al.,[12] who reported the initial isostatic heat of adsorption of 6 kcal mol^{-1} and the mean heat of adsorption of the first four water molecules of 9.6 kcal mol^{-1}, respectively. Vigne-Maeder et al. have also calculated the water−silicalite potential map in which the average energy is expressed as a sum of electrostatic, polarization, dispersion, and repulsion interactions between the atom pairs. The various atomic parameters for the first term are the ab intio results, whereas those of the other terms are empirical. The calculations yield an average water−silicalite interaction at 300 K of −12.5 kcal mol^{-1} and the approximate energy barrier via diffusion through the intersection between the straight and the zigzag channels of the silicalite of 8 kcal mol^{-1}. However, it has been mentioned that the calculated results are very sensitive to the experimental geometry of the silicalite used.

The aim of this study is to use quantum chemical calculations at the Hartree−Fock (HF) and MP2 levels to determine the water−silicalite interactions in order to understand the water orientation, preferable binding sites and energy barrier during the movement into and in the silicalite pores. This framework is the dealuminated analogue of the zeolite type ZSM-5.

2. Calculation Details

2.1. Representation of the Silicalite. The silicalite structure is characterized by two types of channels whose symmetry group is *Pnma*. The crystallographic cell[13] contains 288 atoms, namely 96 Si and 192 O, with cell parameters $a = 20.07$ Å, $b = 19.92$ Å and $c = 13.42$ Å. It is clear that the system consisting of all atoms in the unit cell does not allow the use of quantum chemical calculation, even with a small basis set because of the unreasonable computation time that would be required. Therefore, the silicalite crystal structure was represented by the three fragments (Figure 1b−d), namely single, intersection, and double rings. The sinusoidal and main parts of the straight channels of the crystal (Figure 1a), in which the inner surfaces are almost identical, were represented by the double 10-oxygen-membered ring (Figure 1d). This fragment (mentioned later, for simplicity, as the double ring) consists of 30 O and 22 Si atoms. The larger fragment (35 O and 29 Si atoms) containing both parts of the sinusoidal and straight channels was used to represent the intersection and so-called intersection ring (Figure 1c). Note that the remaining valence orbitals of the silicon atoms of both fragments are then filled up by the hydrogen atoms.

* Corresponding author.
† Chulalongkorn University.
‡ University of Leipzig.

10.1021/jp003337w CCC: $20.00
Published on Web 04/04/2001

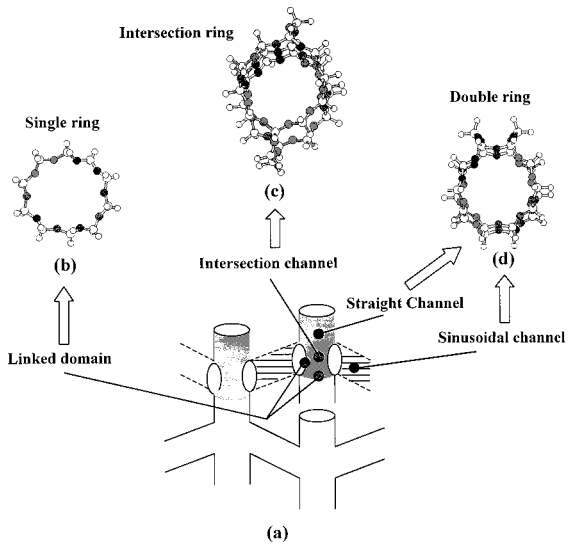

Figure 1. Schematic representations of the (a) silicalite crystal structure, (b) linked domain, (c) straight and sinusoidal channels and (d) intersection channel (for more details see text).

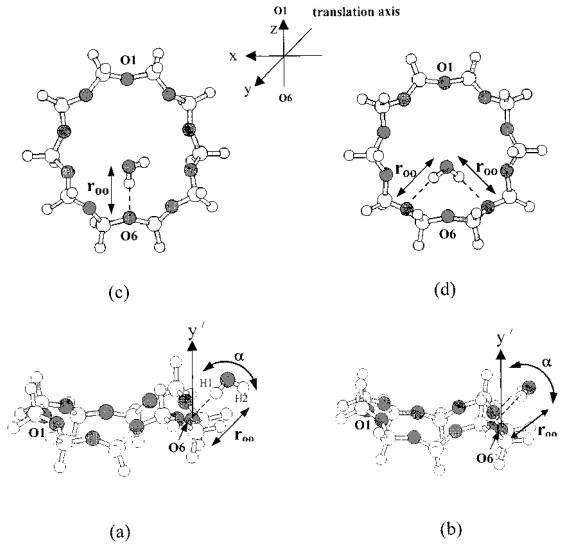

Figure 2. Schematic representations of the binding of water molecule (a)−(b) outside and (c)−(d) inside the silicalite channels (for more details see text).

To investigate the energy barrier for diffusion from the intersection to the straight or to the sinusoidal channels, the water−silicalite interaction in the linked domain has been also calculated. The selected fragment is the 10-oxygen-membered ring (Figure 1b). This fragment, called the single ring, contains 10 O, 10 Si and 20 H atoms.

2.2. Configurations of the Water Molecule. Numerous configurations of water molecules have been generated, varying over -5.0 Å $\leq L \leq 5.0$ Å, $0° \leq \phi_x \leq 360°$and $0° \leq \phi_y, \phi_z \leq 180°$owing to its symmetry, where L is the distance between the oxygen atom of water and the origin of the coordinate system and ϕ_x, ϕ_y, and ϕ_z denote rotational angles around the x, y, and z axes, respectively. The rotational steps are $\Delta\phi_x = \Delta\phi_y = \Delta\phi_z = 15°$ while the translation step is $\Delta L = 1$ Å. The origin of the coordinate system for each fragment is the average of the positions of all oxygen atoms lying on the 10-oxygen-membered rings. The translation or y axis is defined as a vector pointing through the origin and perpendicular to the plane defined by the window of each channel. Then, the z axis is parallel to the vector pointing from O6 to O1 (labeled on the rings shown in Figure 2). Positive or negative distances are determined from the origin to the oxygen atom of the water molecule along the positive or negative translation axis, respectively.

To search for the optimal binding sites both outside and inside the windows, interactions between water and silicalite for each fragment in the four configurations shown in Figure 2 have been calculated. The out-of-plane (Figure 2a−b) and in-plane (Figure 2c−d) configurations are assumed to represent the binding of water to the silicalite framework before and after entering the channels, respectively. For the double hydrogen bond (2HB) configurations (Figure 2b,d), the two O−O distances (r_{OO}) were simultaneously optimized. Inside the pore (Figure 2c,d), the molecular plane of the water molecule was kept parallel to the plane of the 10-oxygen-membered ring (the window plane). For the out-of-plane configurations (Figure 2a,b), we additionally optimized angles y'−O6−Ow (α) as well as rotation around the H_1−Ow bond of water for the single hydrogen bond (1HB) system (Figure 2a), where vector y' is perpendicular to the window plane at O6, Ow denotes the oxygen atom of water, and the H_1−Ow vector points to O6.

2.3. Quantum Chemical Calculations. Ab initio calculations at the HF and the MP2 levels have been performed for the water−silicalite system using extended 6-31G and 6-31G* basis sets.[14,15] Experimental geometries of water[16] and silicalite[13] have been used and kept constant throughout. An error due to the imbalance of the basis set, basis set superposition error (BSSE), has also been examined and taken into consideration. All calculations were performed using the G98 program.[17] All optimizations have been done using the HF method with the 6-31G* basis set with BSSE corrections.

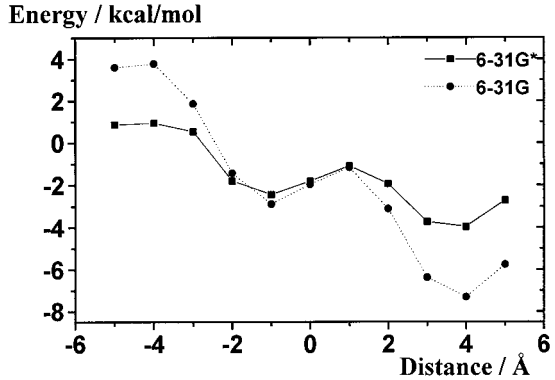

Figure 3. Interaction energy versus water−silicalite distance, calculated using HF method with the 6-31G and 6-31G* basis sets without BSSE corrections for the double-ring framework and a water molecule lying on the translation axis as shown in Figure 2 (for more details see text).

3. Results and Discussion

3.1. Optimal Basis Set, Optimal Method, and Optimal Size of the Fragment. To examine discrepancies due to the method of calculation and the size of the basis set as well as BSSE, the water−silicalite interactions have been calculated for the frameworks of single and double rings using HF and MP2 methods and 6-31G and 6-31G* basis sets with and without BSSE corrections. The calculated results are plotted in Figures 3 and 4.

Figure 3 shows the HF interaction energies between water and silicalite in the double-ring framework, calculated using the 6-31G and 6-31G* basis sets. Both plots exhibit a local minima at $L = -1.0$ Å (L was defined in section 2.2) and the most attractive minimum at $L = 4.0$ Å. The interaction energies obtained from the two basis sets are significantly different,

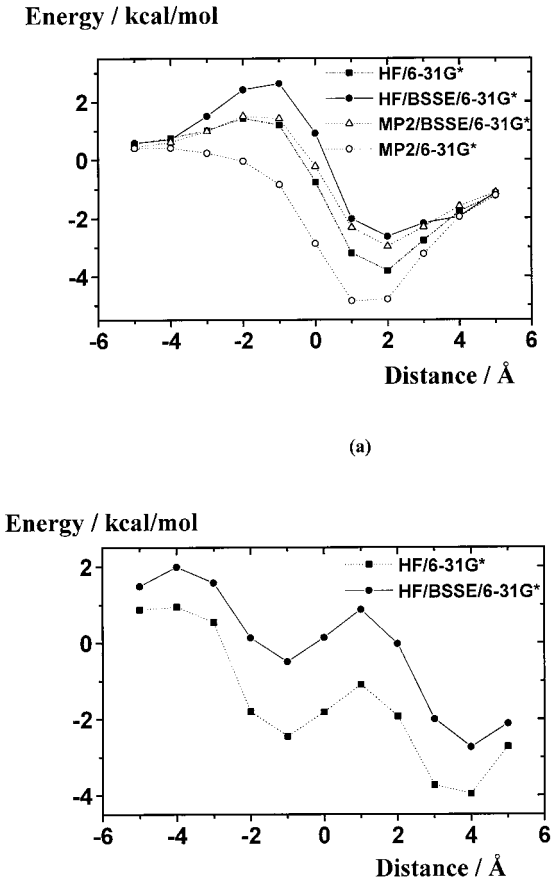

Figure 4. Interaction energy versus water−silicalite distance, calculated using the HF method with the 6-31G* basis set with and without BSSE corrections for the frameworks of (a) single and (b) double rings and a water molecule lying on the translation axis as shown in Figure 2. Results obtained from the MP2 calculations for the framework of a single ring with and without BSSE corrections are also given for comparison (more details see text).

especially in the repulsive and attractive regions where $|L| \geq 2$ Å. As the difference in the interaction energy in both regions is around 100%, it is known that a smaller basis set could be less accurate than a larger one. We therefore conclude that the 6-31G* basis set is substantially more reliable than 6-31G for the investigated system.

Figure 4 displays calculated results for both frameworks, single and double rings, using HF calculations and the 6-31G* basis set with and without BSSE corrections. For the MP2 method, the requirement of computational time for the double ring is not affordable; therefore, the calculations have been performed only for the framework of the single ring, with and without BSSE corrections, and these results are also shown in Figure 4a. It is seen in both figures that there is a rather high error due to the BSSE for both HF and MP2 methods in terms of the interaction energy. For instance, HF and MP2 values at the most attractive region for both single- and double-ring systems amount to an error of about 40% and 100%, respectively. Dependence of the calculated results on the method used can be understood from Figure 4a. The interaction energies including correlation effects based on the MP2 approximation are more stable than those from the HF method. After the correction for BSSE, the effect of the electron correlation is almost negligible, i.e., no significant differences were found between the interaction energies obtained from the two methods for any distance. Another clear conclusion is that although interaction energies from both HF and correlated MP2 methods for single- and double-ring systems suffer from BSSE errors, the two methods are in very good agreement in predicting the geometry of the complex. Note that the difference in the distance to the energy minimum for the frameworks of single ($L = 2.0$ Å) and double ($L = 4.0$ Å) rings are due to different definitions of the origins of the two systems (see section 2.2).

The above observations suggest that correlation methods and BSSE corrections do not play a role regarding the predicted geometry of the system. However, to increase the reliability of the derived interaction energies, all data points reported in this study are the results of HF calculations with BSSE corrections.

In addition to the above results, Figure 4 also contains information on the optimal size of the fragment, which is used to represent the silicalite. Taking into account the definition of the origin, the difference in the optimal interaction energies taking place at 2.0 and 4.0 Å for the frameworks of single and double rings, respectively, is almost negligible. This fact is valid for the results obtained both before and after BSSE corrections. For instance, the interaction energy after the BSSE correction at $L = -3.0$ Å for the framework of single ring and at $L = -5.0$ Å for that of the double ring are almost identical (about 1.5 kcal mol^{-1}). The corresponding values before the BSSE correction for the single and the double rings are 1.0 and 0.7 kcal mol^{-1}, respectively. Therefore, a clear and useful conclusion is that the framework of a single 10-oxygen-membered ring is already large enough to represent the silicalite crystal structure in the investigation of the water−silicalite interaction energy.

3.2. Optimal Diffusion Route. *(i) Diffusion through the center of the window*. On the basis of the conclusions of section 3.1, HF calculations with the 6-31G* basis set and BSSE correction have been carried out for the three fragments. For each system, numerous water−framework configurations have been generated by varying L, ϕ_x, ϕ_y, and ϕ_z as described in section 2.2. Results for four main routes defined by the $\{\Delta\phi_x, \Delta\phi_y, \Delta\phi_z\}$ coordinates of {0, 0, 0}, {0, 90, 0}, {180, 0, 0}, and {180, 90, 0} have been displayed in Figure 5. The optimal route, in which the energy minimum for each distance takes place, has been also given for all plots. The areas inside the pores for the three fragments have been estimated and labeled as the regions between the two vertical-dot lines (Figure 5a,c). These ranges for the single, double, and intersection rings are -0.5 Å $\leq L \leq 0.5$ Å, -1.5 Å $\leq L \leq 1.5$ Å, and -2.5 Å $\leq L \leq 2,5$ Å, respectively.

The plots for all fragments indicate clearly how the water molecule moves and turns via diffusion along the translation axis (Figure 2) through the center of the channel. The water molecule starts to interact with the window of the silicalite at a long distance, far from the molecular center. The preferred configuration at this distance is to point its dipole vector toward the center of the pore (graphs 3 and 4 for all plots of Figure 5). Then the water molecule leaves the pore by pointing its dipole vector toward the center of the channel (graphs 1 and 2). In addition, the interaction energy in the region around center of the pore of the intersection ring (Figure 5c), -1.0 Å $\leq L \leq 3.0$ Å, is strongly orientation dependent. It is interesting to note here that the energy gap between two plots of parallel dipole moments, graphs 1 and 2 or graphs 3 and 4 as shown in Figure 5b, is higher than that seen in Figures 5a and 5c. This leads us to conclude that the energy barriers for the rotation around the dipole axis of the water molecule in the straight and the sinusoidal channels (represented by a double ring) are higher than those of the intersection channel and the linked domain.

It can be also seen from Figure 5 that the diffusion of a water molecule along the translation axis through the center of a

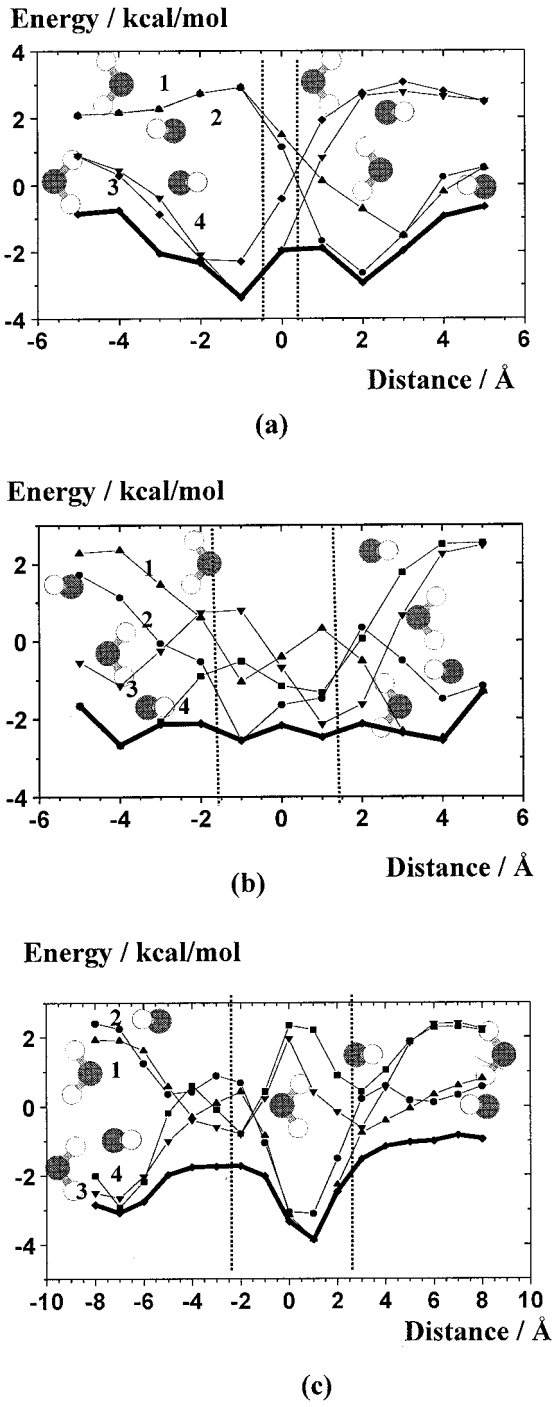

Figure 5. Interaction energy versus water−silicalite distance, calculated using the HF method with the 6-31G* basis set and BSSE corrections for the frameworks of (a) single, (b) double, and (c) intersection rings and a water molecule lying on the translation axis in the configurations given in the insert; $l = \{0,90,0\}$; $n = \{0,0,0\}$; $s = \{180,0,0\}$; $t = \{180,90,0\}$. The bold solid-lines represent the optimal route. An area between the two vertical dot-lines is estimated to be inside the pore (more details see text).

window of the silicalite is a kind of rolling movement. The molecule must move and turn in order to find the optimal route (bold-solid lines in Figure 5a,c). As the energy fluctuation on the optimal route for the double ring (Figure 5b) is much lower than those of the other fragments. Change of the interaction energies during the diffusion into and in the channel along the optimal route is within thermal fluctuations at room temperature, which amounts to about 0.6 kcal mol^{-1}. This led to a clear conclusion that the motion of a water molecule in the straight and the sinusoidal channels is rather smooth compared to that in the linked domain and the intersection channel.

TABLE 1: Optimal Binding Distance (r_{OO} in Å), Angle (α in Degree), and Interaction Energy (ΔE in kcal mol^{-1}) Obtained from the Geometry Optimization Using 6-31G* Basis Set with BSSE Corrections for the Water−Silicalite Complexes in the Four Configurations (a), (b), (c), and (d), which Corresponds to Those Shown in Figures 2a−d, Respectively

configuration	fragment	single ring	double ring	intersection ring
(a)	r_{OO}	3.93	3.91	3.48
	a	79.9	47.5	101.3
	ΔE	−2.61	3.67	−0.35
(b)	r_{OO}	3.64	3.66	3.52
	a	60.3	52.8	96.4
	ΔE	−1.32	−1.02	0.84
(c)	r_{OO}	3.42	3.51	3.59
	ΔE	0.34	−0.95	−0.4
(d)	r_{OO}	3.69	3.60	3.83
	ΔE	−0.81	−0.98	−1.04

(ii) Diffusion along the Inner Wall. Another possible pathway for the water molecule to diffuse in the silicalite channel is to attach to a specific binding site on the window, then enter the pore, find the next binding site, and move from one site to another along the inner wall of the channel. Such information can be calculated using the supramolecular approach as described in detail in section 2.3 and as schematically displayed in Figure 2. The obtained optimization energies and corresponding distances are summarized in Table 1.

The following information can be extracted from the interaction data given in Table 1: (I) The most stable binding site for the water molecule before entering into the silicalite channel is to coordinate to the oxygen atom of the linked domain to form a single hydrogen bond outside the pore (Figure 2a). The corresponding interaction energy of −2.61 kcal mol^{-1} is comparable to those when a water molecule moves along the optimal route (Figure 5a). Therefore, the water molecule can enter the pore via the linked domain either by using the optimal route at the center of other pore or by binding to the window as a single hydrogen bond. The situations are different for the double and the intersection fragments. To enter the pore through the optimal route is much more favorable than when the molecule binds to the framework. (ii) To bind to the inner wall, the interaction energies obtained from the three fragments fluctuate within a thermal limit at room temperature. This implies no preferential binding site for water molecule in the inner wall of the silicalite pores. The observed result supports the fact that the silicalite channel is hydrophobic. (iii) The interaction energy between the water molecule and the inner wall as mentioned above is less attractive compared to that when the water molecule moves along the optimal route through center of the pore (Figure 5). These data indicate clearly that the diffusion in the silicalite pore takes place via the optimal route (Figure 5).

3.3. Energy Barrier to Enter the Channel. The energy change (ΔE_{net}) for a water molecule to enter the silicalite channel is simply defined as the difference between the most stable water−silicalite interaction energies inside (ΔE_{in}^{min}) and outside (ΔE_{out}^{min}) the pores. According to our model, the possible pathways for entering the single fragment are either to bind to the framework first or to move along the optimal route via the central line; only the second pathway is preferable for the double and the intersection fragments. However, the most stable interaction energy to bind a water molecule to the single ring outside the pore (Figure 2a) of −2.61 kcal mol^{-1} is higher than

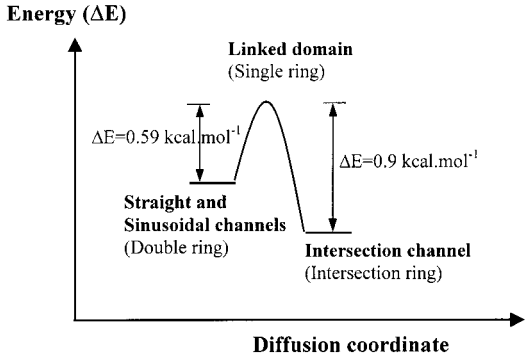

Figure 6. Changes of the water−silicalite interaction energy via diffusion in the silicalite channels.

TABLE 2: The Water−Silicalite Interaction Energies (kcal mol^{-1}) along the Optimal Route Taken from the Corresponding *L* Distance: ΔE_{out}^{min}, ΔE_{in}^{min}, and ΔE_{max} Are the Minimum Outside the Pore, the Minimum Inside the Pore, and the Maximum that Lies between the ΔE_{out}^{min} and ΔE_{in}^{min}, Respectively (more details see text)

fragment	ΔE_{out}^{min}	ΔE_{max}	ΔE_{in}^{min}	$\Delta E_{barrier}$	ΔE_{net}
single ring	−3.58 ($L = -1$ Å)	−1.96 ($L = 0$ Å)	−1.96 ($L = 0$ Å)	1.62	1.62
double ring	−2.79 ($L = -4$ Å)	−2.12 ($L = -2$ Å)	−2.55 ($L = -1$ Å)	0.67.	0.24
intersection ring	−3.14 ($L = -7$ Å)	−1.86 ($L = -2$ Å)	−3.86 ($L = 1$ Å)	1.28	−0.72

that to move the molecule along the optimal route of −3.58 kcal mol^{-1} taking place at $L = -1$ Å (Figure 5a). Therefore, the energy change and the energy barrier for all fragments have been calculated only when a water molecule moves along the optimal route. The results are summarized in Table 2.

The maximum of the interaction energy (ΔE_{max}), which lies between the ΔE_{in}^{min} and ΔE_{out}^{min} on the optimal route, suggests how easily a water can enter the pore via this pathway. The energy barrier ($\Delta E_{barrier}$) for the water molecule to enter the pore can then be expressed as $\Delta E_{max} - \Delta E_{out}^{min}$, resulting in the values of 1.62, 0.67, and 1.28 kcal mol^{-1} for the single, double, and intersection rings, respectively.

The energy data in Table 1 indicate clearly that the energy barrier of about 1.5 kcal mol^{-1} is required to drive the water molecule to enter the pore of the silicalite, the linked domain (represented by the single ring) and the intersection channel (represented by the intersection ring). The situation is different for entering the straight and the sinusoidal channels (represented by the double ring), i.e., a water molecule enters these channels via the optimal route without energy barrier (0.6 kcal mol^{-1} is within a thermal fluctuation of room temperature).

In terms of energy change, the ΔE_{net}, which defines as $\Delta E_{in}^{min} - \Delta E_{out}^{min}$ (Table 2) indicates clearly that entering the linked domain and the intersection channel are endothermic and exothermic processes, respectively. On the other hand, the energy change for this process is almost zero for the straight and the sinusoidal channels.

3.4. Energy Barrier to Diffuse across the Channels. To investigate the energy barrier for a water molecule to diffuse from one to another channel inside the silicalite, the most stable interaction energies for encapsulation of water molecules in the three channels, shown in Table 1, are considered and the diffusion process is schematically drawn in Figure 6. The small barrier takes place only when a water molecule crosses the linked domain, which is represented by the single ring (Figures 1a and 1b) to and from the intersection channels. The energy requirement of 0.96 kcal mol^{-1} is equivalent to a temperature of about 450 K. This value is much less than that of 8 kcal mol^{-1} obtained from the development of the water−silicalite potential map using an empirical method.[12]

Some comments can be made concerning the encapsulation energy shown in Table 1, in which the most stable position takes place in the intersection channel. This observation is different from that reported theoretically for the light alkane molecules, which stated that they bind more strongly in the straight or sinusoidal than in the intersection channels.[18−23] Therefore, it is suggested by these results that the degree of hydrophobicity, typical character of the silicalite, of the intersection channel is less than those of the other channels. In addition, our value for the encapsulation energy of the water molecule in the silicalite pore of −3.9 kcal mol^{-1} is much higher than the expermental value of −9.6 kcal mol^{-1} and the calculated value of −12.5 kcal mol^{-1} reported by Vigne-Maeder et al.[12] However, it should be noted here, therefore, that the two values given in ref. (12) are too strong to represent the interaction energy between a polar molecule such as a water and the hydrophobic channels of the silicalite. This statement was supported by the simulation results published recently by Takabe et al.[24] The simulated results for the water−methanol mixture in the silicalite membrance show that no water molecule diffuses into the silicalite pore. Adsorption takes place only with the silanol groups on the external surface. Therefore, a strongly experimental heat of adsorption is a consequence of the adsorption on the surface but not in the hydrophobic micropore of the silicalite. However, preliminary result by Kärger[25] using PFG-NMR measurement indicates the diffusion of water molecule in the silicalite micropore at high temperatures.

Acknowledgment. Computing facilities provided by the Austrian−Thai Center for Chemical Education and Research at Chulalongkorn University, the National Electronic and Computer Technology Center, Bangkok, Thailand, and the Computing Center at Leipzig University are gratefully acknowledged. This work was supported financially by the Thailand Research Fund (TRF) and the Deutscher Akademischer Austauschdienst (DAAD). C.B. acknowledges the DAAD-Royal Golden Jubilee Scholarships, Grant No. A/99/16872. The Royal Golden Jubilee Scholarships, Grant. No. PHD/0090/2541and Des Duetschen Forschungsemeinschaft, Grant No. SFB294 are as well acknowledged by all authors. R.H. thanks Fondues der Chemischen Industrie, Frankfurt. The authors thank Professor Keiji Morokuma, Professor Jörg Kärger, and PD Dr. Siegfried Fritzsche for helpful comments and suggestions and Dr. David Ruffolo for proofreading the manuscript.

References and Notes

(1) Breck, D. W. *Zeolite Molecular Sieves*; Wiley: New York, 1974.
(2) Kärger, J.; Ruthven, D. M. *Diffusion in Zeolites and Other Microporous Solids*; Wiley: New York, 1992.
(3) Rao, C. N. R.; Natarajan, S.; Neeraj, S. *J. Am. Chem. Soc.* **2000**, *122*, 2810.
(4) Davis, M. E. *Microporous Mesoporous Mater.* **1998**, *21*, 173.
(5) Singh, A. P.; Kale, S. M. *Catal. Today* **1999**, *49*, 245.
(6) Demontis, P.; Suffritti, G. B.; Tilocca, A. *J. Phys. Chem. B*, **1999**, *103*, 8141.
(7) Vlugt, T. J. H.; Krishna R.; Smit, B. *J. Phys. Chem. B* **1999**, *103*, 1102.
(8) Haberlandt, R. *Thin Solid Films* **1998**, *330*, 34.
(9) Mikhailenko, S. D.; Kaliaguine, S.; Ghali, E. *Microporous Mater.* **1997**, *11*, 37.
(10) Komiyama, M.; Kobayashi, M. *J. Phys. Chem. B* **1999**, *103*, 10651.
(11) Flanigen, E. M.; Bennett, J. M.; Grose, R. W. *Nature* **1978**, *271*, 512.
(12) Vigné-Maeder F.; Auroux, A. *J. Phys. Chem.* **1990**, *94*, 314.

(13) Olson, D. H.; Kokotailo, G. T.; Lawton, S. L.; Meier, W. M. *J. Phys. Chem.* **1981**, *85*, 2238.
(14) Hehre, W. J.; Random, L.; Schleyer, P. v. R.; Pople, J. A. *Ab Initio Molecular Orbital Theory*; Wiley: New York, 1987.
(15) Francl, M. M.; Petro, W. J.; Hehre, W. J.; Binkley, J. S.; Gordon, M. S.; Defrees, D. J.; Pople, J. A. *J. Chem. Phys.* **1982**, *77*, 3654.
(16) Benedict, W. S.; Gailar, N.; Plyler, E. K. *J. Chem. Phys.* **1956**, *24*, 1139.
(17) Frisch, M. J.; Trucks, G. W.; Head-Gordon, M.; Gill, P. M. W.; Wong, M. W.; Foresman, J. B.; Johnson, B. G.; Schlegel, H. B.; Robb, M. A.; Replogle, E. S.; Gomperts, R.; Andres, J. L.; Raghavachari, K.; Binkley, J. S.; Gonzalez, C.; Martin, R. L.; Fox, D. J.; Defrees, D. J.; Baker, J.; Stewart, J. J. P.; Pople, J. A. *Gaussian 98*, Revision A, Gaussian, Inc., Pittsburgh, PA, 1998.
(18) June, L. R.; Bell, A. T.; Theodorou, D. N. *J. Phys. Chem.* **1990**, *94*, 1508.
(19) June, L. R.; Bell, A. T.; Theodorou, D. N. *J. Phys. Chem.* **1992**, *96*, 1051.
(20) Nicholas, J. B.; Trouw, F. R.; Mertz, J. E.; Iton, L. E.; Hopfinger, A. J. *J. Phys. Chem.* **1993**, *97*, 4149.
(21) Zhu, W.; Van de Graaf, J. M.; Van den Broeke, L. P. J.; Kapteijn, F.; Moulijn, J. A. *Ind. Eng. Chem. Res.* **1998**, *37*, 1934.
(22) Gergidis, L. N.; Theodorou, D. N. *J. Phys. Chem.* **1999**, *103*, 3380.
(23) Vlugt, T. J. H.; Krishna, R.; Smit, B. *J. Phys. Chem. B* **1999**, *103*, 1102.
(24) Takaba, H.; Koyama, A.; Nakao, S. I. *J. Phys. Chem.* **2000**, *104*, 6353.
(25) Kärger, J. unpublished data.